

PUBLISHED VERSION

Douglass, M.; Bezak, E.

Physical modelling of proton and heavy ion radiation using Geant4, *Heavy Ion Accelerator Symposium on Fundamental and Applied Science 2012, 2012* / Evers, M., Kluth, P., Tims, S.G., Wallner, A., Williams, E. (ed./s), pp.04001-1-04001-5.

© Owned by the authors, published by EDP Sciences, 2012.

This is an Open Access article distributed under the terms of the Creative Commons Attribution License 2.0, which permits unrestricted use, distribution and reproduction in any medium, provided the original work is properly cited.

PERMISSIONS

<http://www.epj-conferences.org/for-authors/copyright>

COPYRIGHT

Copyright on any article in *EPJ Web of Conferences* is retained by the author(s) under the [Creative Commons Attribution license](#), which permits unrestricted use, distribution, and reproduction in any medium, provided the original work is properly cited.

19th January 2015

<http://hdl.handle.net/2440/88736>

Physical Modelling of Proton and Heavy Ion Radiation using Geant4

M. Douglass^{1,2}, E. Bezak^{1,2}

¹School of Chemistry and Physics, University of Adelaide, North Terrace, Adelaide, South Australia

²Department of Medical Physics, Royal Adelaide Hospital, North Terrace, Adelaide South Australia

Abstract. Protons and heavy ion particles are considered to be ideal particles for use in external beam radiotherapy due to superior properties of the dose distribution that results when these particles are incident externally and due to their relative biological effectiveness. While significant research has been performed into the properties and physical dose characteristics of heavy ions, the nuclear reactions (direct and fragmentation) undergone by He⁴, C¹² and Ne²⁰ nuclei used in radiotherapy in materials other than water is still largely unexplored. In the current project, input code was developed for the Monte Carlo toolkit Geant 4 version 9.3 to simulate the transport of several mono-energetic heavy ions through water. The relative dose contributions from secondary particles and nuclear fragments originating from the primary particles were investigated for each ion in both water and dense bone (ICRU) media. The results indicated that the relative contribution to the total physical dose from nuclear fragments increased with both increasing particle mass and with increasing medium density. In the case of 150 MeV protons, secondary particles were shown to contribute less than 0.5% of the peak dose and as high as 25% when using 10570 MeV neon ions in bone. When water was substituted for a bone medium, the contributions from fragments increased by more than 6% for C¹² and Ne²⁰.

1 Introduction

It has been demonstrated that the use of protons and heavy ions for the treatment of cancer results in relatively large doses being administered to the tumour region while minimising the damage of healthy tissue surrounding it. This effect is enhanced by the higher relative biological effectiveness of heavy ions at low energies (high linear energy transfer). As a result the relative dose in the region of healthy tissue surrounding the tumour region can be minimised by lowering the physical dose to the target region while still achieving the same level of biological damage due to the higher RBE [1].

In this paper we demonstrate that as much as 25% of the total physical dose when using heavy ions originates from secondary particles produced in nuclear interactions between the primary ion beam and the medium in which it is propagating. Common secondary particles formed when using a primary proton beam are: alpha particles, helium-3 nuclei, neutrons and deuterons [2]. In the case of protons, the contribution from secondary particles only becomes significant beyond the distal edge of the Bragg peak. When using more massive and energetic heavy ions, the contribution from secondary particles is significant even within the plateau region of the heavy ion dose distribution. Low mass fragments produced in nuclear reactions may gain a large fraction of the primary particles energy enabling them to

travel beyond the Bragg peak depositing their energy in this region.

2 Methods and Materials

In the current work, the Monte Carlo toolkit “Geant 4” was used to simulate the formation and transport of fragments produced through fragmentation reactions and their contributions to the total physical dose were analysed before and after the Bragg peak.

This research was performed using Geant 4 Version 9.3. The input code (physics list) was developed during the current research to enable protons and heavy ions to be used as primary particles. The physics list was also designed to simulate appropriate physical interactions for all common secondary particles. The Binary Cascade model was used and tested as the nuclear interaction model for both proton and heavy ions [3]. Simulated measurements were made using the G4ScoringMesh class and a rectangular detector was used with a voxel size of 0.16 cm (slice thickness in direction of z-axis) unless otherwise specified.

The primary particles (mono-energetic pencil beam) were then fired into the 10 x 10 x 50 cm³ water and bone phantom at the edge of the phantom. The region surrounding the water phantom was a vacuum. Energies of each of the primary particles were chosen to give a Bragg peak at the same depth as the 150 MeV Proton

Beam. For protons of this energy, hadronic interactions become significant in comparison to ionisation energy losses. At this energy, protons have maximum range of approximately 15.8 cm in water. Hence, all other particle energies were chosen to produce a Bragg peak depth of approximately 16 cm in both water and bone media. The input code was configured in the first instance to fire protons and heavy ions into the water and bone media with the resultant physical dose in the phantom filtered by individual fragments. The filter was then modified to record the energy spectra of secondary neutrons in an attempt to determine the level of risk associated with neutron radiation originating from heavy ion radiation. The physical dose characteristics of each particle were compared in water and bone media as tumours are often treated adjacent to higher density materials in the body which may significantly alter the final dose profile of the beam.

The selection of primary ions used in these simulations spans the range of heavy ions used at present in hadron therapy (protons – neon). Neon has been shown to be the upper limit for heavy ions used in radiotherapy [4] as the physical dose distribution does not change significantly for ions with an atomic greater than 10.

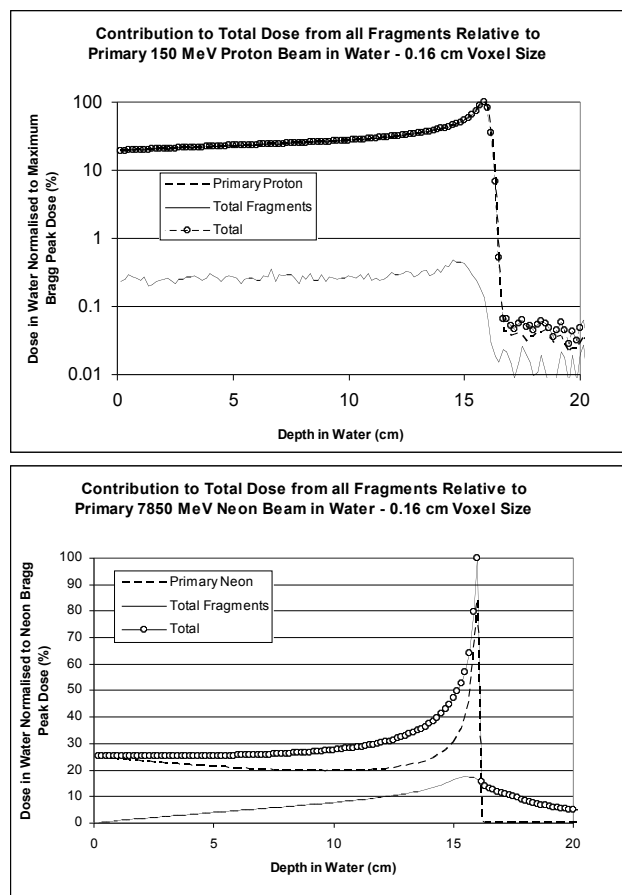
The statistical uncertainty due to the Monte Carlo process in the results was estimated using seven identical simulations in which 50,000 primary C^{12} ions were fired into a water medium. Each simulation was run using a different random number seed producing seven different yet similar results. The standard deviation between the results was calculated. The maximum uncertainty occurred at the Bragg peak with a maximum value of 1.4%.

Using the Geant 4 Monte Carlo Code, the contribution to the total dose in water from the primary heavy ion nuclei and nuclear fragments was measured for four primary ions: 150 MeV protons, 600 MeV alpha, 3500 MeV C^{12} and 7850 MeV Ne^{20} .

3 Results

The contribution to the physical dose due to all fragments was first considered for the four ions. When 150 MeV protons were used, secondary particles produced in nuclear reactions contributed less than 0.5% of the maximum dose in the Bragg peak as illustrated in figure 1(a). Of all the secondary particles tracked in the simulation, the most significant secondary particles were alpha particles which contributed a maximum of 0.19% of the dose at the Bragg peak followed by secondary protons with 0.12%.

The simulation was repeated for alpha particles (figure 1(b)) of energy 600 MeV. Maximum recorded contributions from secondary particles and fragments were 2.5% of the maximum dose. When using alpha particles as the primary source, secondary protons were the most significant secondary particle contributing a maximum of 1.47% of the maximum dose in the Bragg peak. Beyond the distal edge of the Bragg peak, the physical dose contribution from secondary protons was recorded at depths beyond 18 cm to be two orders of



Figures 1. The physical dose contribution (normalised to Primary Ion Bragg Peak Dose (%)) of (a) 150 MeV proton, (b) 600 MeV alpha particle and (c) 3500 MeV carbon and (d) 7850 MeV neon Ion source (10^5 primary particles), the relative contributions from nuclear fragments and the total physical dose deposited in water originating from the primary ion particles.

magnitude larger than the primary alpha particles. This dose is still less than 0.5 % of the dose in the Bragg peak and hence is still negligible compared with the dose in the plateau and Bragg peak region of the dose distribution.

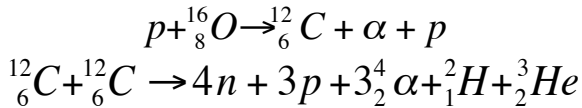
Figure 1(c) shows fragmentation contributions to the total dose distribution originating from a 3500 MeV C^{12} beam. Using particles of these energies and masses results in the relative contribution from nuclear fragments becoming more significant. The maximum contribution from secondary particles was 12.5% and occurred just before the Bragg peak position at a depth of approximately 15.5 cm. The relatively large contribution from fragments produces a characteristic “tail” of dose beyond the distal edge of the Bragg peak where the relative dose of nuclear fragments to the primary C^{12} beam is approximately three orders of magnitude larger. These contributions are now significant beyond the Bragg peak with the dose due to fragments still as large as 8.3% beyond the distal edge of the Bragg peak.

The last type of ions investigated were 7850 MeV Ne^{20} ions. Figure 1(d) shows the contributions from secondary particles and fragments originating from the primary 7850 MeV neon source. The contribution from fragments increased to approximately 17.5% at a depth of 15.5 cm. Beyond the Bragg peak, the relative dose of

fragments to the primary neon beam was up to 5 times that present in the previous simulation with carbon. Fragment contribution remained as high as 13% of the maximum dose beyond the distal edge of the Bragg peak.

When using 3500 MeV C^{12} ions, analysis into individual fragments showed that C^{11} and C^{10} were the most significant nuclear fragments contributing up to 6% of the maximum dose. Such fragments would be formed when one or two outer orbital nucleons were removed in a stripping reaction of the primary C^{12} nucleus and the target nuclei in the water medium. More complex fragmentation reactions resulted in the next most significant fragments which were isotopes of Boron contributing 4% of the maximum dose. This indicates that only a small number of nucleons are removed from the primary nucleus in such reactions. These results are consistent with the results obtained in [5].

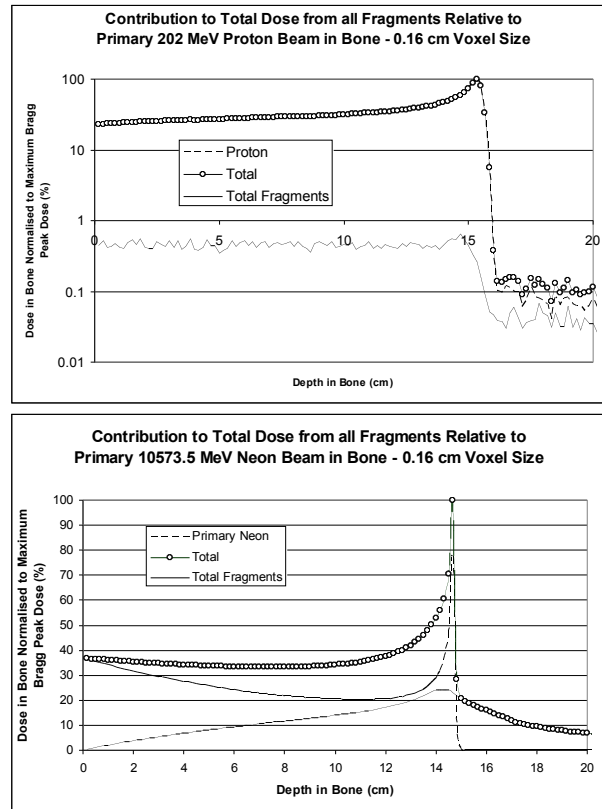
Table 1. Example of common (a) and an extreme case (b) of fragmentation. Reactions observed in Geant4 simulation.



When using a 3500 MeV C^{12} beam, the most significant nuclear fragments are other isotopes of carbon and boron isotopes contributing 6% and 4% of the maximum Bragg peak dose respectively. However, beyond the Bragg peak at depths of up to 30 cm (15 cm beyond the Bragg peak) isotopes of hydrogen and helium (including secondary protons, deuterons, tritons and alpha particles) produce a physical dose of over 1% of the Bragg peak dose in this region. This is the origin of the dose “tail” present in the dose distribution of heavier ions. With carbon and alpha particles typically having RBE values of ten [6] or greater and four respectively there is potential for inaccurate dose distribution in a patient undergoing carbon radiotherapy.

When using 7850 MeV neon ions in water, he proportion of more massive fragments produced in set reactions has increased. The highest contributing fragments are oxygen, neon and fluorine each contributing 4.1 %, 4.0% and 3.5% of the maximum dose respectively.

When using primary neon ions of such energies, before the Bragg peak, the most common reactions are ones in which the primary neon ion loses only one to four of the nucleons in a collision leaving the original fragment with the majority of the initial energy. However, in such reactions, the individual nucleons or small nuclei produced at shallow depths carry a significant fraction of the initial energy of the primary neon ions enabling them to propagate well beyond the Bragg peak before coming to a complete stop. Hence, smaller isotopes such as hydrogen, helium, lithium and beryllium contribute most significantly to the dose beyond the Bragg peak (combined dose as large as 2.0% of the Bragg peak dose).



Figures 2. The dose contribution (normalised to Primary Ion Bragg Peak Dose (%)) of 200 MeV proton, 810 MeV alpha particle and 4714 MeV carbon and 10570 MeV

Protons with energies of approximately 200 MeV in a compact bone medium were first considered. The first change which resulted from the new medium was an increase in dose contribution from secondaries to 0.65% compared with less than 0.5% in water shown in figure 2. Again, the most significant secondary particles were alpha particles contributing 0.28% of the maximum dose. This indicates that for the purposes of external beam radiotherapy, the change in dose from secondary fragments resulting from nuclear interactions of protons with water (similarly soft tissue) and bone are insignificant.

In the case of alpha particles, the changes in the dose distribution were more significant. Total fragment contributions increased from 2.5 % in water to approximately 6 % in bone as shown in figure 2(b). Similarly in bone, the most significant secondary particles were protons contributing a maximum of 2.8% to the maximum dose.

Fragment contribution increased when using C^{12} ions in bone compared with water. Figure 2(c) illustrates that total contributions increased from 12.5% in water to 22% in bone. Largest contributions before the Bragg peak were from secondary carbon and boron ions contributing 8.2% and 5.5% respectively to the maximum dose. Secondary hydrogen and helium fragments contributed most strongly beyond the Bragg peak with contributions as high as 1.5% of the Bragg peak dose at depths of 30 cm (twice the depth of the Bragg peak).

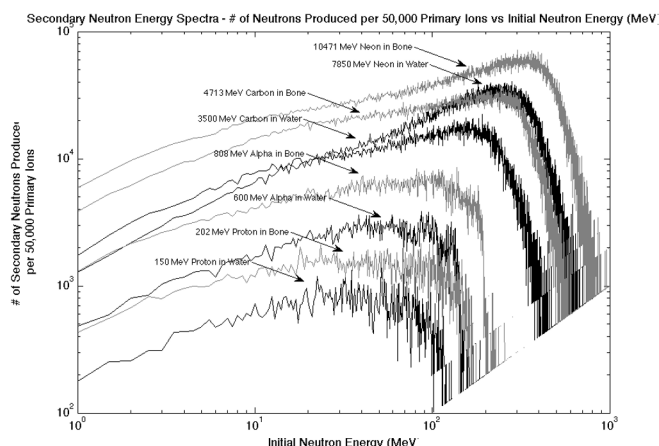


Figure 3. Energy spectra of secondary neutrons due to interactions of protons and heavy ions in water and dense bone media. Energy vs number of neutrons per 50,000 primary ions.

Figure 2(d) shows the contributions from all significant secondary nuclear fragments resulting from the collision of 10573.5 MeV Ne^{20} ions in bone. Total fragment contributions increased to a total of 25% compared with 17.5% in water. Similarly in bone, the largest secondary contributions to the total dose originate from large fragments of the original neon nucleus. Isotopes of oxygen, neon, fluorine and nitrogen contributed 5.3%, 4.8%, 4.3% and 3.9% to the maximum dose respectively and were formed in smaller stripping reactions resulting from the loss of between 1 and 6 nucleons from the primary neon nucleus.

3.1 Comparison of Secondary Neutron Spectra in Water and Dense Bone Media

Biological damage incurred from secondary neutron radiation is a concern not only in heavy ion radiotherapy but also when using photons. Neutron radiation is of particular concern as it has a low interaction cross section at high energies (highly penetrating radiation) and an RBE of up to twenty when it approaches thermal energies [7] making it highly detrimental to organic cells.

The energy spectra of neutrons between 0 and 1000 MeV were simulated and compared in water and bone originating from each ion tested previously. The energy spectra of secondary neutrons in both water and bone were simulated using 2000 energy bins of width 0.5 MeV between 0 and 1000 MeV with the number of neutrons recorded in each range.

Figure 3 illustrates that the energy of peak neutron intensity increases with both particle energy, particle charge and the target material. While the relative number of neutrons is much higher for carbon and neon, the energy of peak neutron intensity is greatly skewed towards higher energies resulting in the majority of the neutron radiation being significantly less damaging (low RBE at high energies).

At low energies, there is a significant increase in neutron intensity when heavier ions are used. Neutron intensity at an energy of 1 MeV (RBE of 20) increases by a factor of 2.5, 10, 7.5 for alpha particles, carbon ions and neon ions respectively. When the medium is switched to

bone neutron intensity increases by a factor of 2, 10, 20 and 30 for protons, alpha particles, carbon and neon in bone respectively compared with protons in water. These results indicate that treatment of a region containing dense bone material may result in adverse biological effects to tissue beyond this region due to the high level of neutron radiation.

4 Conclusion

Based on the results of the simulations above, it is apparent that both the density of the material, the type and initial energy of the heavy ion has a significant effect on the number of fragmentation reactions which occur and the overall contribution to the total physical dose.

The results also indicate that the largest fraction of fragmentation reactions result in a small number of nucleons (1-6 nucleons) from either the target or projectile nucleus being ejected in “abrasion” reactions [8] rather than the nucleus being obliterated. These processes produce low mass ions which carry large fractions of the original ion’s energy enabling them to propagate over twice the distance of the Bragg peak position. It has been confirmed [9] that this is the origin of the dose “tail” present beyond the distal edge of the Bragg peak when heavy ions are used. Consistently, the particles primarily responsible for the physical dose in this region were lighter ions such as secondary protons (and other hydrogen ions) and alpha particles. The significance of such a result is that when heavy ions are used to treat tumours adjacent to radiosensitive organs (i.e. the spinal cord), such organs will receive a relatively large physical dose (up to 10% of Bragg peak dose), which would otherwise be spared with the use of protons which do not undergo nuclear fragmentation.

The number of neutrons produced per primary ion was shown to increase with primary particle energy and charge and the density of the material in which it is propagating. Since a large fraction of the total number of secondary neutrons produced in hadronic interactions have energies corresponding to high RBE values (RBE of 20 at 1 MeV) there is a potential risk to the patient due to neutron radiation damage.

When we also consider that contributions from fragments increases with increasing primary particle mass and the RBE of the fragments is dependant on the atomic number of the secondary ions [10], carbon ions appear to be the optimal choice for use in heavy ion radiotherapy as this ion produces a relatively small distal dose compared with ions with $Z > 6$ and the RBE at the Bragg peak is very high compared with $Z < 6$.

References

1. Paganetti, H., Olko, P., Kobus, H., Becker, R., Schmitz, T., Waligorski, M., et al., 1997, Calculation of the Relative Biological Effectiveness for proton Beams using Biological Weighting Functions., *Radiation Oncology, Biology and Physics*, (1997) 37 (3)

2. Paganetti, H, 2002 , Nuclear Interactions in proton Therapy, Dose and Relative Biological Effect Distributions Originating from Primary and Secondary Particles. *Physics in Medicine and Biology* , (2002). 47, 747-764.
3. Apostolakis et. Al 2009, Progress in Hadronic Physics Modelling in Geant4, *Journal of Physics: Conference Series*, 160(1)
4. Oliver Jäkel, Introduction to medical physics aspects of Hadron therapy, *Radiotherapy and Oncology*, Volume 73, Supplement 2, December 2004, Page 63
5. Zhao Qiang, Zhang Feng-Shou, Wang Zhi-Ping, Zhou Hong-Yu, Secondary Beam Fragments Produced by 200 and 400MeV/u $^{12}\text{C}^{6+}$ Ions in Water, CHINESE. PHYS. LETT. Vol. 26, No. 9 (2009) 092501
6. Ando K, Kase Y, Biological characteristics of carbon-ion therapy,. *International Journal of Radiation Biology*, Vol. 85, No. 9, pp. 715–728
7. Eric J. Hall , RBE and OER Values as a Function of Neutron Energy, *Euwp.& Cancer* Vol. 10, pp. 297-299. Pergamon Press 1974.
8. K Gunzert-Marx, H Iwase, D Schardt and R S Simon, Secondary beam fragments produced by 200MeV/u ^{12}C ions in water and their dose contributions in carbon ion radiotherapy, - *New Journal of Physics* 10 (2008) 075003 (21pp)
9. Igor Pshenichnov, Alexander Botvina, Igor Mishustin, Walter Greiner, Nuclear fragmentation reactions in extended media studied with Geant4 toolkit, *Nucl. Instr. and Meth. in Phys. Res. B*, 2009
10. D. Schardt, Tumor therapy with high-energy carbon ion beams, *Nuclear Physics A* 787 (2007) 633c–641c
11. A.N. Golovchenko, J. Skvar, R. Ili, L. Sihver, V.P. Bamblevski, S.P. Tretyakova, D. Schardt, R.K. Tripathi, J.W. Wilson, R. Bimbot, Fragmentation of 200 and 244 MeV/u carbon beams in thick tissue-like absorbers, *Nuclear Instruments and Methods in Physics Research B* 159 (1999) 233-240
12. G. Kraft ,Tumor Therapy with Heavy Charged Particles, *Progress in Particle and Nuclear Physics* 45 (2000) 473-544 .
13. W. K. Weyrather, G. Kraft, RBE of carbon ions: Experimental data and the strategy of RBE calculation for treatment planning, *Radiotherapy and Oncology*, Volume 73, Supplement 2, December 2004, Pages 161-169